

Verification of Genetic Differences and Immune Cell Infiltration Subtypes in Neuroblastoma Tumor Microenvironment for Immunotherapy

Bo Qian (✉ boqian@njmu.edu.cn)

NMU: Nanjing Medical University <https://orcid.org/0000-0002-1081-6471>

Jing Sun

Children's Hospital of Nanjing Medical University

Pengcheng Zuo

Children's Hospital of Nanjing Medical University

Min Da

Children's Hospital of Nanjing Medical University

Xuming Mo

Children's Hospital of Nanjing Medical University

Yongjun Fang

Children's Hospital of Nanjing Medical University

Research

Keywords: neuroblastoma, immune cell infiltration, Immunotherapy, biomarker, prognosis.

Posted Date: August 17th, 2021

DOI: <https://doi.org/10.21203/rs.3.rs-789623/v1>

License: © ⓘ This work is licensed under a Creative Commons Attribution 4.0 International License.

[Read Full License](#)

Abstract

Background: The tumor microenvironment (TME) has achieved remarkable results in the research of cancer progression in the past few years. It is crucial to understand the nature and function of TME in tumors because of precise treatment strategies for individual cancers having received widespread attention, including immunotherapy. The immune infiltrative profiles of neuroblastoma (NB) have not yet been completely illustrated. The purpose of this research is to analyze tumor immune cell infiltration (ICI) in the microenvironment of NB.

Methods: We applied CIBERSORT and ESTIMATE algorithms to evaluate the ICI status of 438 NB samples. Three ICI models were selected and ICI scores were acquired. Subgroups with high ICI scores based on immune activation signaling pathways have better overall survival.

Results: The genes of immunosuppressive glycosaminoglycan biosynthesis heparan sulfate signaling pathway were markedly enriched in the low ICI score subgroup. It was inferred that compared with low ICI NB subtypes, patients with high ICI NB subtypes were more likely to respond to immunotherapy and a better prognosis.

Conclusion: Notably, our ICI scores not only provided new clinical and theoretical basis for mining NB prognostic markers related to the microenvironment, but also aided new ideas for the development of new NB precision immunotherapy methods.

Introduction

Neuroblastoma (NB) is an extracranial malignant solid tumor derived from the embryonic neural crest cells, its mortality accounts for nearly 15% of all pediatric tumors [1, 2]. The age of onset of NB is usually early, and the median age at diagnosis is 17 months. It usually occurs in the adrenal medulla or paravertebral ganglia, so it can locate in the abdominal cavity, thoracic cavity, neck, etc. About half of NB patients have stage distant metastases at the first diagnosis [3]. Although the five-year survival rate of low-risk NB is greater than 95%, the five-year survival rate of high-risk is still less than 50% after comprehensive treatment such as surgery, radiotherapy, chemotherapy and biological therapy, because of its later recurrence, distant metastasis, and drug resistance [4].

Over the last decades, various immunotherapies have been applied to treat more and more refractory malignant cancers [5]. Immunotherapy methods related to neuroblastoma treatment have been expected to become the most promising treatment strategy, providing a new direction for its treatment. However, immunotherapeutic strategies benefit only a subset of patients, while most patients face the problem of resistance to immunotherapy [6]. With the insights into the immune system and tumor microenvironment, new targets may facilitate NB patients for immunotherapy treatment.

High risk NB has a high degree of malignancy and is resistant to radiotherapy and chemotherapy. Therefore, new treatment strategies are needed to improve their biological behavior. The tumor-specific

antigen and immune microenvironment phenotype may be used as predictive indicators for evaluating the effect of immunotherapy. Tumor microenvironment (TME) is a dynamic system formed by the interaction of cancer cells with tumor interstitial cells, immune cells, extracellular matrix, surrounding vascular tissues, and signaling molecules [7]. In addition to the invasion, migration, and proliferation of tumor cells, tumor metastasis is also closely related to its microenvironment. The inhibitory changes and heterogeneity of TME are important factors that promote tumor progression and affect immune efficacy [8–9]. Due to multiple factors such as immunosuppressive microenvironment and lack of tumor-specific antigen expression, the high-risk group NB is not sensitive to immunotherapy and belongs to cold tumor, while low-risk group NB has the features of hot tumor. Increased expression of tumor-associated macrophages M2 (CD163+) could decrease function of NK cells, DCs and T cells in these cold tumors [10]. The main components of infiltrating stromal cells are macrophages and fibroblasts. The cell-to-cell interaction between tumor-associated macrophages M2 and Cancer-associated fibroblasts promotes the progression of neuroblastoma by mutual induction of recruitment and activation. Studies have confirmed that these cells promote tumor-promoting activity by activating the ERK1/2 and STAT3 signaling pathways in neuroblastoma cells [11]. These cells, called CAFs-MSCs, promote the proliferation of NB cells and secrete a variety of inflammatory cytokines and chemokines to enhance resistance to chemotherapy, such as IL-6, IL-8, VEGF-A, CCL-2 And CXCL12. The Disialoganglioside (GD2) was highly expressed in NB cells, resulting in the immune function of T cells impaired and immunotherapy resistance [12]. Programmed death 1(PD-1), the main immune checkpoint receptor, expressed on human T cells, dendritic cells and natural killer T cells, while programmed death ligand 1 (PD-L1) was expressed on the surface of NB cells. The PD-1/PD-L1 pathway inhibits the proliferation and differentiation of T cells after PD-1 binds to the PD-L1 of NB cells, then induce activated T cells to transform into non-effect T cells or apoptosis [13–14].

Next generation sequencing (NGS) has become an important part of precise tumor diagnosis and treatment that used in multiple aspects such as the detection of driver genes related to tumor targeted therapy, the analysis of drug resistance mechanisms, the evaluation of cancer metastasis and prognosis, and the full dynamic monitoring of tumor patients. CIBERSORT is a tool that uses a deconvolution algorithm to predict the proportion of cells. It can analyze the cellular composition of immune tissues based on standardized expression data and energize the abundance of specific cell types [15–16]. In this study, we explored the gene expression of TARGET-NB and GSE85047 to get a comprehensive overview of the tumor immunity by two calculation algorithms (CIBERSORT and ESTIMATE) [17]. Then we divided NB into different discrete subtypes by immune cell infiltration mode [18]. Besides, we divided NB into different discrete subtypes by immune cell infiltration mode. Establishing the ICI score to characterize various immune characteristics could promote the best choice for NB patients who respond to immunotherapy.

Methods

Neuroblastoma Data collection

The RNA data (level 3) in TARGET Data were downloaded from the Therapeutically Applicable Research to Generate Effective Treatments (TARGET)-NB database (<https://ocg.cancer.gov/programs/target/data-matrix>). The Affymetrix microarray data sets GSE85047 were obtained from Gene Expression Omnibus (GEO, <http://www.ncbi.nlm.nih.gov/geo>) database. Clinical data such as age, INSS, survival and outcome were also downloaded from TARGET and GEO, respectively. Fragments per kilobase of transcripts per million (FPKM) data from the TARGET samples were converted to transcripts per million (TPM). In order to obtain key information from these expression matrices, Perl scripts and R software (R-project.org) were used to merge and preprocess the original data. If the gene symbol corresponds to multiple probe IDs, the average value of the probes was calculated as the expression level of the gene.

Immune score determination for the NB microenvironment and immune cellular fraction estimates

We calculated the immune score of NB with the ESTIMATE algorithm. All patients were classified into high group and low group according to their immune/matrix score. The CIBERSORT algorithm was used to evaluate tumor infiltrating immune cell (TIIC) data in NB samples from the TARGET and GEO cohorts [19–20]. The visualization of the results was completed by using the R packages. The hierarchical agglomerative clustering of NB was performed according to the ICI mode of all patients. This analysis was executed using the R package and repeated 1000 times to ensure the stability of the classification.

Differentially expressed genes (DEGs)-related with the ICI clusters

Patients were classified into different ICI clusters base on immune-cell infiltration. Absolute fold change > 1 and $p < 0.05$ (after adjustment) were determined by setting the cut-off criterion for DEGs. Data was applied to analysis by package edge R [18].

Pathway and function enrichment analysis

Functional enrichment analysis of immune-cell infiltration-related DEGs was performed with the "clusterProfiler" R package to identify the Gene Ontology (GO) and Kyoto Encyclopedia of Genes and Genomes (KEGG). P value < 0.05 was considered as the critical cutoff [21].

Principal component analysis (PCA)

PCA is a statistical method that applies the idea of dimensionality reduction to transform multiple variables into a few uncorrelated comprehensive variables [22]. We performed PCA to define the differences in infiltrating immune cells among distinct groups. The diagram of PCA could classify different infiltrating immune cells as variables to describe the differences in NB samples.

Statistical Analyzes

All statistical analyses were performed using SPSS 22.0 software. Kaplan-Meier analysis was conducted to detect the survival curve of the subgroups in the data set. The log-rank test assessed statistically

significant differences. The Wilcoxon test was performed to compare the two groups, while the Kruskal-Wallis test was applied to compare more than two groups.

Results

The profile of Immuno-cell Infiltration in the TME of NB

The study design was shown in Fig. 1. In our study, we firstly adopted the two algorithms (ESTIMATE and CIBERSORT) to analyze the immune cells subtype with R platform in NB samples. Subsequently, the ConsusClusterPlus package was performed unsupervised clustering of 438 NB samples from GSE85047 and [TARGET]-NB) to define different subgroups.

The Kaplan-Meier curves indicated that ICI A and ICI B were not significantly associated with improved outcome (log rank test, $p = 0.179$; Fig. 2A-C). Then we calculated the immune cell subtype in R platform between the two ICI Subtypes.

The relative content of resting dendritic cells in all samples were nearly 0. Between these two main immune subtypes, the immune cells found in the ICI cluster A mainly comprised high ImmuneScore, naive B cells, T cells regulatory (Tregs), naive CD4 T cells and CD8 T cells, while the samples in the ICI cluster B were represented with a significantly higher density of StromalScore, T cells CD4 memory resting, M0, M2 macrophages and Mast cells resting (Fig. 2D). In addition, the heat map of correlation coefficients of NB TME was analyzed (Fig. 2E). We found that the relative content of M2 cells in NB samples was significantly negatively correlated with those cells (CD8 T cells, naive B cells, T cells regulatory).

Identified Immune Gene Subtype

After the gene datasets from TARGET-NBL and GSE85047 samples were integrated with R (version 3.6.1), we identified an aggregate of 117 DEGs by limma package. Then we divided these samples into three genomes based on DEGs and called them gene clusters A-C (Fig. 3A). There were 24 DEGs significantly positively related to the gene cluster were named ICI gene features A, while the remaining DEGs were called ICI gene features B. Dimension reduction was used to reduce interference by Boruta algorithm. The heatmap of the 117 DEGs in R software was drawn to show the correlation between the genomic traits and clinical features (Fig. 3B) [23]. The enrichment analyses by the GO term and KEGG pathway were showed in Figs. 3C and 3D. The ICI features genes A included neutrophil activation involved in immune response, ficolin - 1-rich granule and neutrophil degranulation; while ICI features genes B gene were associated with extracellular matrix structural constituent, collagen-containing extracellular matrix and extracellular structure organization.

In addition, the Survival and survminer package of R software were performed to explore the relationship between survival feature and ICI gene clusters. The Kaplan-Meier analysis revealed that the samples in gene cluster A were significantly associated with improved outcome, while samples in remaining gene clusters had a poor prognosis (log rank test, $p = 0.040$; Fig. 3E). The gene cluster C was characterized by more abundant stromal cell infiltration and immunosuppression-related M2 macrophages, suggesting

that the result of immunotherapy was unfavorable [24–25]. The expression of PD-L1 and CTLA4 were significantly different in these three genome clusters (Kruskal-Wallis, $p < 0.001$; Fig. 2G and 2H). Compared with ICI gene clusters A and C, CTLA4 and PD-L1 had the lowest expression levels in ICI gene cluster B.

Construction of the ICI Score

We performed principal component analysis (PCA) to calculate the quantitative indicators of different ICI subtypes, which were labeled as ICI scores A and B, respectively. Then, we obtained prognostic-related score defined as ICI scores and divided the patients in the TARGET and GSE85047 cohorts into high or low ICI scores subgroup. The distribution of different patients in diverse gene clusters was summary by the Alluvial graph (Fig. 4A). The Gene ICI cluster A that expressed a higher ICI scores was significantly related to an improved survival outcomes of 72.3% (136/188), while the samples in the gene ICI cluster B expressed a less high ICI scores witnessed a lower overall survival outcome (58.2%, 131/225). Then we analyzed the relationship between the immune tolerance of the NB patients and the prognostic value of the ICI score. A few representative immune activity-related targets (such as PD-L1, CTLA4, LAG3, IDO1 and HAVCR2) and immune checkpoint-related targets were selected [26–27]. In our study, Exception of LAG3, all selected immune activity-related targets and immune checkpoint-related targets were remarkably overexpressed in the high ICI group. The gene set enrichment analysis (GSEA) showed that the glycosaminoglycan biosynthesis heparan sulfate signaling pathway was associated with the low ICI score group, while apoptosis, cytokine receptor interaction, toll like receptor and leukocyte transendothelial migration signaling pathways were associated with the high ICI group (Figs. 4C and 4D). The Kaplan-Meier analysis revealed that the samples in high ICI score subtype were significantly associated with better outcome, while samples in low ICI score subtype had a unfavorable OS ($p = 0.025$; Fig. 4E).

Discussion

Immunotherapy have shown encouraging results and may improve the survival status and quality of high-risk NB patients [13–14]. However, the inconsistency of their exploratory study of tumor surface markers highlights the necessity of determining the ideal subgroup of NB immunotherapy, which is still a major challenge in immunotherapy. A monoclonal antibody named dinutuximab attached to GD2 on the surface of neuroblastoma cells has been performed as an immunotherapy drug for the neuroblastoma [6]. Recently, various evidence has confirmed the potential of PD-1/PD-L1 in immunotherapy of neuroblastoma [28–29]. However, only a small percentage of patients benefit from immunotherapy. Therefore, it is important to identify those subgroups that can benefit from immunotherapy. In our research, we validated a method that can quantify the integrated tumor microenvironment in NB. Our results indicated that the ICI score was not only an effective prognostic feature, but also been used to identify NB patients that could benefit from immunotherapy.

As in previous studies, patients with specific active immunity have a significantly better prognosis, while high-risk NB patients with immune cell dysfunction increased immune resistance, resulting in tumor

progression and unfavorable prognosis [30–31]. At first, we analyzed the ICI from 438 NB sample cohorts in two databases and divided NB into two different immune subtypes. The results displayed that the relative content of resting dendritic cells in all samples was nearly zero. ICI cluster A was marked by high ImmuneScore, naive B cells, T cells regulatory (Tregs), naive CD4 T cells and CD8 T cells. The samples in the ICI cluster B were represented with a significantly higher expression of StromalScore, T cells CD4 memory resting, M0 and M2 macrophages, and Mast cells resting. Although the Kaplan-Meier survival curves was not statistically significant.

Studies have shown that a number of cytokines, TME components and the host's immune response have a positive impact on the anti-tumor response and maintain a dynamic balance. These molecular changes during tumorigenesis may interfere with the function of infiltrating immune cells, resulting in the destruction of the dynamic balance between immune tolerance and activity [32].

We utilized the combination of ICI and immune associated gene expression as a new method for patient-specific customized treatment strategies. Then, the novelty immune-related genes based on the significant ICI gene clusters were used to explore its prognostic significance by integrating ICI gene clusters with survival information. The Kaplan-Meier analysis revealed that the samples in gene cluster A were significantly associated with improved outcome, while samples in remaining gene clusters had a poor prognosis (log rank test, $p = 0.040$; Fig. 2E). Patients the lowest expression of immune score and matrix score are grouped in ICI gene cluster B subtype, which are related to the immune cold phenotype. While patients with ICI gene cluster A and C subtypes showed higher inflammatory cell density and immune scores. Moreover, we found that the increased expression of M2 macrophage infiltration in ICI gene cluster C subtype was related to high stromal score, meaning an unfavorable prognosis [25]. Compared with other subtypes, samples ICI gene cluster A subtype are associated with a good prognosis, which could benefit from immunotherapy.

There is an urgent need to quantify the ICI pattern of neuroblastoma because of the heterogeneity of the individual microenvironment. Similar individual models have been well established in colorectal cancer, head and neck squamous cell carcinoma and breast cancer to improve prediction accuracy [18, 33–34].

The potential "signature subtype" was established to quantify the ICI model in our study. The Kaplan-Meier analysis showed that the samples high ICI score subtype was significantly associated with better outcome, while samples in low ICI score subtype had an unfavorable OS (log rank test, $p = 0.025$). The most immune checkpoint associated targets and immune activity associated targets were overexpressed in the high ICI subgroup. It is inferred that compared with ICI NB subtypes, patients with high ICI NB subtypes were more likely to respond to immunotherapy. For example, PD-1/PD-L1 targeted immunotherapy was more likely to be effective because of the PD-L1 expression was more expressed in the high ICI NB subgroup. The genes of immunosuppressive glycosaminoglycan biosynthesis heparan sulfate signaling pathway were remarkably enriched in the low ICI score subgroup by GSEA analysis. Destroying the integrity of the extracellular matrix and basement membrane was the primary condition for the invasion and metastasis of malignant tumors. Microscopic damage on the extracellular matrix in

the tumor microenvironment is a sign of tumor aggressive growth [35]. Heparanase (HPSE), as an endogenous endoglycosidase, was highly expressed in high-risk neuroblastoma. Tumor cells secreted a large amount of heparanase to destroy the strong network structure of extracellular matrix and basement membrane, promoting the invasion and metastasis of inflammatory cells and tumor cells and related diseases Progress [36]. In the high ICI group, Apoptosis, Cytokine receptor interaction, Toll like receptor and Leukocyte transendothelial migration signaling pathways were enriched.

Conclusion

In summary, it is urgent to constantly explore novel prognostic markers for the treatment of tumor, we found that ICI score presented here is applicable in NB and can also be used for development of specific prognostic biomarkers. We found that differences in ICI subtypes are related to individual heterogeneity and treatment efficacy. In addition, it can help develop new ideas for NB immunotherapy methods.

Abbreviations

TME
the tumor microenvironment; NB:neuroblastoma; ICI:immune cell infiltration; OS:overall survival; GD2:disialoganglioside; PD-1:programmed death 1; PD-L1:programmed death ligand 1; NGS:Next generation sequencing; DEGs:differentially expressed genes; PCA:principal component analysis.

Declarations

Acknowledgements

Not applicable.

Author Contributions

Bo Qian, Xuming Mo and Yongjun Fang designed the study. Pengcheng Zuo, Min Da and Bo Qian collected the samples and performed the clinical information. Bo Qian and Jing Sun performed the bioinformatics analysis of neuroblastoma data. Bo Qian drafted the manuscript, and Xuming Mo and Yongjun Fang made further revisions. All authors read and approved the final version of the manuscript.

Ethics approval and consent to participate

Not applicable.

Consent for publication

Not applicable.

Availability of data and materials

The data used to support the findings of this study are included within the article

Competing interests

The authors declare that they have no competing interests.

Funding

This research was supported by the National Natural Science Foundation of China (81670155, 81903383), Scientific Research Projects of Jiangsu Health Commission (ZDB2020018).

Publisher's Note

Springer Nature remains neutral with regard to jurisdictional claims in published maps and institutional affiliations.

Author details

¹Department of Cardiothoracic Surgery, Children's Hospital of Nanjing Medical University, Nanjing, China.

²Department of Hematology and Oncology, Children's Hospital of Nanjing Medical University, Nanjing, China.

References

1. Uemura S, Ishida T, Thwin KKM, Yamamoto N, Tamura A, Kishimoto K, et al. Dynamics of Minimal Residual Disease in Neuroblastoma Patients. *Front Oncol.* 2019;9:455.
2. Esposito MR, Aveic S, Seydel A, Tonini GP. Neuroblastoma treatment in the post-genomic era. *J Biomed Sci.* 2017;24(1):14.
3. Ho WL, Hsu WM, Huang MC, Kadomatsu K, Nakagawara A. Protein glycosylation in cancers and its potential therapeutic applications in neuroblastoma. *J Hematol Oncol.* 2016;9(1):100.
4. Boboila S, Lopez G, Yu J, Banerjee D, Kadenhe-Chiweshe A, Connolly EP, et al. Transcription factor activating protein 4 is synthetically lethal and a master regulator of MYCN-amplified neuroblastoma. *Oncogene.* 2018;37(40):5451–65.
5. He Y, Jiang Z, Chen C, Wang X. Classification of triple-negative breast cancers based on Immunogenomic profiling. *J Exp Clin Cancer Res.* 2018;37(1):327.
6. Park JA, Cheung NV. Targets and Antibody Formats for Immunotherapy of Neuroblastoma. *J Clin Oncol.* 2020;38(16):1836–48.
7. Wu T, Dai Y. Tumor microenvironment and therapeutic response. *Cancer Lett.* 2017;387:61–8.
8. Zeng D, Zhou R, Yu Y, Luo Y, Zhang J, Sun H, et al. Gene expression profiles for a prognostic immunoscore in gastric cancer. *Br J Surg.* 2018;105(10):1338–48.

9. Jiang Y, Zhang Q, Hu Y, Li T, Yu J, Zhao L, et al. ImmunoScore Signature: A Prognostic and Predictive Tool in Gastric Cancer. *Ann Surg*. 2018;267(3):504–13.
10. Pelizzo G, Veschi V, Mantelli M, Croce S, Di Benedetto V, D'Angelo P, et al. Microenvironment in neuroblastoma: isolation and characterization of tumor-derived mesenchymal stromal cells. *BMC Cancer*. 2018;18(1):1176.
11. Borriello L, Nakata R, Sheard MA, Fernandez GE, Sposto R, Malvar J, et al. Cancer-Associated Fibroblasts Share Characteristics and Protumorigenic Activity with Mesenchymal Stromal Cells. *Cancer Res*. 2017;77(18):5142–57.
12. Perdicchio M, Ilarregui JM, Verstege MI, Cornelissen LA, Schetters ST, Engels S, et al. Sialic acid-modified antigens impose tolerance via inhibition of T-cell proliferation and de novo induction of regulatory T cells. *Proc Natl Acad Sci U S A*. 2016;113(12):3329–34.
13. Nallasamy P, Chava S, Verma SS, Mishra S, Gorantla S, Coulter DW, et al. PD-L1, inflammation, non-coding RNAs, and neuroblastoma: Immuno-oncology perspective. *Semin Cancer Biol*. 2018;52(Pt 2):53–65.
14. Dondero A, Pastorino F, Della Chiesa M, Corrias MV, Morandi F, Pistoia V, et al. PD-L1 expression in metastatic neuroblastoma as an additional mechanism for limiting immune surveillance. *Oncoimmunology*. 2016;5(1):e1064578.
15. Newman AM, Liu CL, Green MR, Gentles AJ, Feng W, Xu Y, et al. Robust enumeration of cell subsets from tissue expression profiles. *Nat Methods*. 2015;12(5):453–7.
16. Gentles AJ, Newman AM, Liu CL, Bratman SV, Feng W, Kim D, et al. The prognostic landscape of genes and infiltrating immune cells across human cancers. *Nat Med*. 2015;21(8):938–45.
17. Yoshihara K, Shahmoradgoli M, Martinez E, Vegesna R, Kim H, Torres-Garcia W, et al. Inferring tumour purity and stromal and immune cell admixture from expression data. *Nat Commun*. 2013;4:2612.
18. Zhang X, Shi M, Chen T, Zhang B. Characterization of the Immune Cell Infiltration Landscape in Head and Neck Squamous Cell Carcinoma to Aid Immunotherapy. *Mol Ther Nucleic Acids*. 2020;22:298–309.
19. Zhang C, Zheng JH, Lin ZH, Lv HY, Ye ZM, Chen YP, et al. Profiles of immune cell infiltration and immune-related genes in the tumor microenvironment of osteosarcoma. *Aging*. 2020;12(4):3486–501.
20. Pan H, Lu L, Cui J, Yang Y, Wang Z, Fan X. Immunological analyses reveal an immune subtype of uveal melanoma with a poor prognosis. *Aging*. 2020;12(2):1446–64.
21. Liberzon A, Subramanian A, Pinchback R, Thorvaldsdottir H, Tamayo P, Mesirov JP. Molecular signatures database (MSigDB) 3.0. *Bioinformatics*. 2011;27(12):1739–40.
22. Zhao W, Wang D, Zhao J, Zhao W. Bioinformatic analysis of retinal gene function and expression in diabetic rats. *Exp Ther Med*. 2017;14(3):2485–92.
23. Yu G, Wang LG, Han Y, He QY. clusterProfiler: an R package for comparing biological themes among gene clusters. *OMICS*. 2012;16(5):284–7.

24. Chen YP, Wang YQ, Lv JW, Li YQ, Chua MLK, Le QT, et al. Identification and validation of novel microenvironment-based immune molecular subgroups of head and neck squamous cell carcinoma: implications for immunotherapy. *Ann Oncol.* 2019;30(1):68–75.
25. Biswas SK, Mantovani A. Macrophage plasticity and interaction with lymphocyte subsets: cancer as a paradigm. *Nat Immunol.* 2010;11(10):889–96.
26. Hugo W, Zaretsky JM, Sun L, Song C, Moreno BH, Hu-Lieskovan S, et al. Genomic and Transcriptomic Features of Response to Anti-PD-1 Therapy in Metastatic Melanoma. *Cell.* 2016;165(1):35–44.
27. Ayers M, Lunceford J, Nebozhyn M, Murphy E, Loboda A, Kaufman DR, et al. IFN-gamma-related mRNA profile predicts clinical response to PD-1 blockade. *J Clin Invest.* 2017;127(8):2930–40.
28. Eissler N, Mao Y, Brodin D, Reutersward P, Andersson Svahn H, Johnsen JI, et al. Regulation of myeloid cells by activated T cells determines the efficacy of PD-1 blockade. *Oncoimmunology.* 2016;5(12):e1232222.
29. Boes M, Meyer-Wentrup F. TLR3 triggering regulates PD-L1 (CD274) expression in human neuroblastoma cells. *Cancer Lett.* 2015;361(1):49–56.
30. Voeller J, Erbe AK, Slowinski J, Rasmussen K, Carlson PM, Hoefges A, et al. Combined innate and adaptive immunotherapy overcomes resistance of immunologically cold syngeneic murine neuroblastoma to checkpoint inhibition. *J Immunother Cancer.* 2019;7(1):344.
31. Borriello L, Seeger RC, Asgharzadeh S, DeClerck YA. More than the genes, the tumor microenvironment in neuroblastoma. *Cancer Lett.* 2016;380(1):304–14.
32. Chen DS, Mellman I. Elements of cancer immunity and the cancer-immune set point. *Nature.* 2017;541(7637):321–30.
33. Bramsen JB, Rasmussen MH, Ongen H, Mattesen TB, Orntoft MW, Arnadottir SS, et al. Molecular-Subtype-Specific Biomarkers Improve Prediction of Prognosis in Colorectal Cancer. *Cell Rep.* 2017;19(6):1268–80.
34. Callari M, Cappelletti V, D'Aiuto F, Musella V, Lembo A, Petel F, et al. Subtype-Specific Metagene-Based Prediction of Outcome after Neoadjuvant and Adjuvant Treatment in Breast Cancer. *Clin Cancer Res.* 2016;22(2):337–45.
35. Qu H, Zheng L, Pu J, Mei H, Xiang X, Zhao X, et al. miRNA-558 promotes tumorigenesis and aggressiveness of neuroblastoma cells through activating the transcription of heparanase. *Hum Mol Genet.* 2015;24(9):2539–51.
36. Ramani VC, Purushothaman A, Stewart MD, Thompson CA, Vlodaysky I, Au JL, et al. The heparanase/syndecan-1 axis in cancer: mechanisms and therapies. *FEBS J.* 2013;280(10):2294–306.

Figures

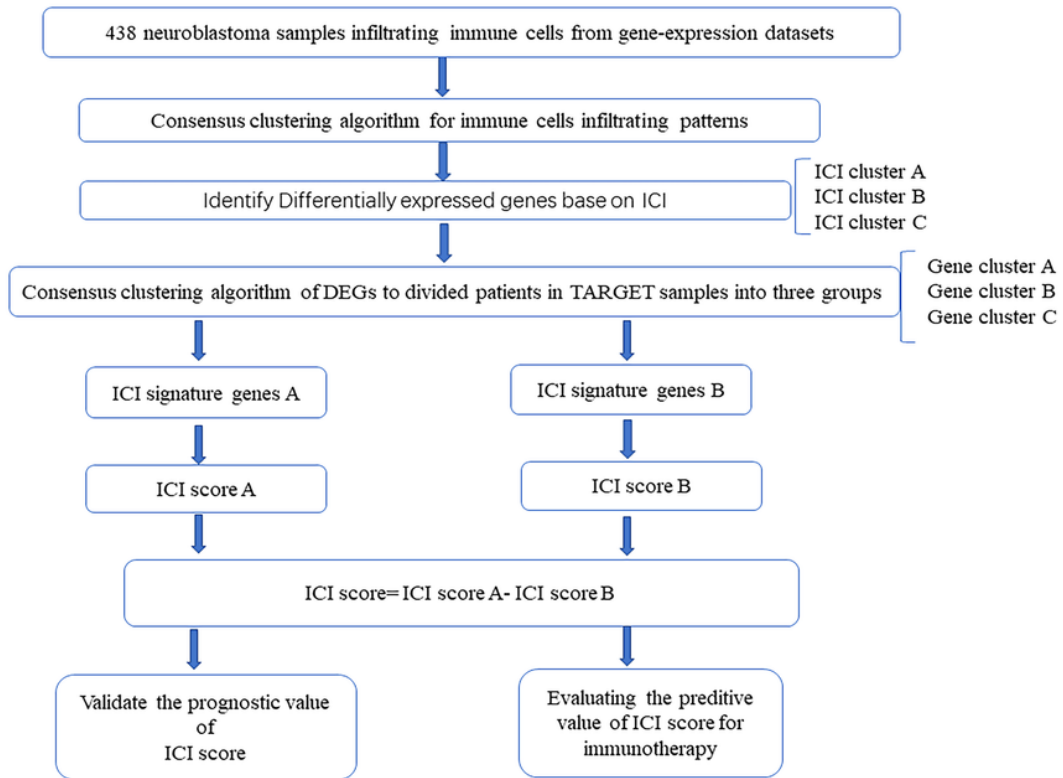


Figure 1

Summary of study design.

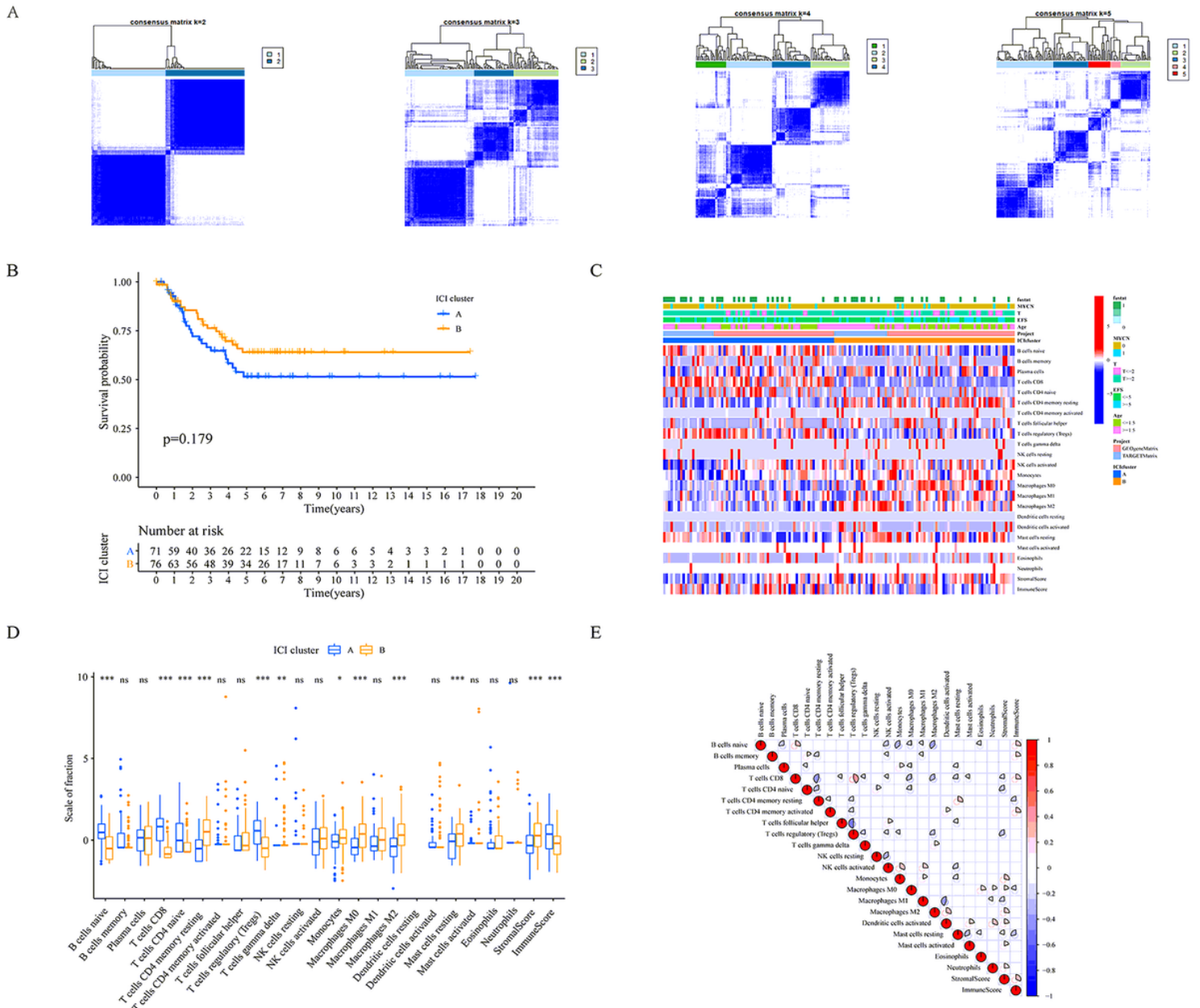


Figure 2

The profiles of Immuno-cell Infiltration in the TME of NB. (A) undergoes 1000 hierarchical clustering to determine the stable k value of the consensus matrix for all NB patients ($k = 2-5$). (B) Association between tumor-associated immune cells in NB patients and overall survival ($p = 0.179$). (C) The distribution of infiltrating immune cells in different NB groups. (D) Kruskal-Wallis was used to test the differences in infiltrating immune cells, immune scores and matrix scores in different ICI clusters. NS no significance; *** $p < 0.001$; ** $p < 0.01$; * $p < 0.05$. (E) The interreaction of tumor-related infiltrating immune cells in NB.

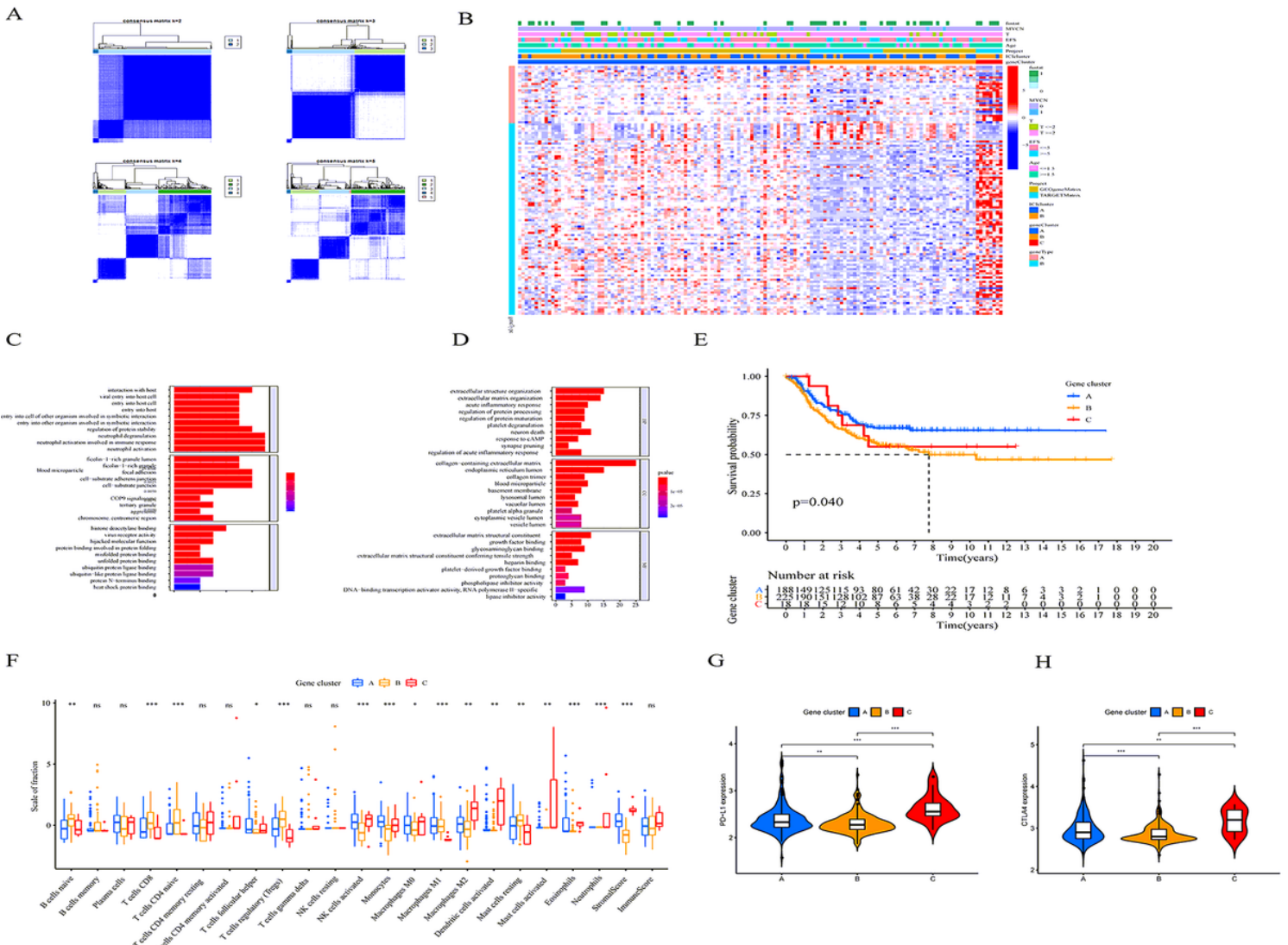


Figure 3

The distinguish of immune-related gene subtype. (A) The DEG in different groups was divided into three groups by unsupervised cluster analysis: gene cluster A-C. (B) The distribution of infiltrating immune cells in different NB subtypes. (C and D) Gene ontology (GO) enrichment analysis of notable genes of different ICI subtypes: ICI notable genes. (E) Association between different NB subgroups and overall survival, $p = 0.04$. (F) Differences in infiltrating immune cells, immune scores and matrix scores of different NB gene subtypes. NS no significance; *** $p < 0.001$; ** $p < 0.01$; * $p < 0.05$. (G-H) The distribution of CTLA4 and PD-L1 expression among different ICI genotypes ($p < 0.001$)

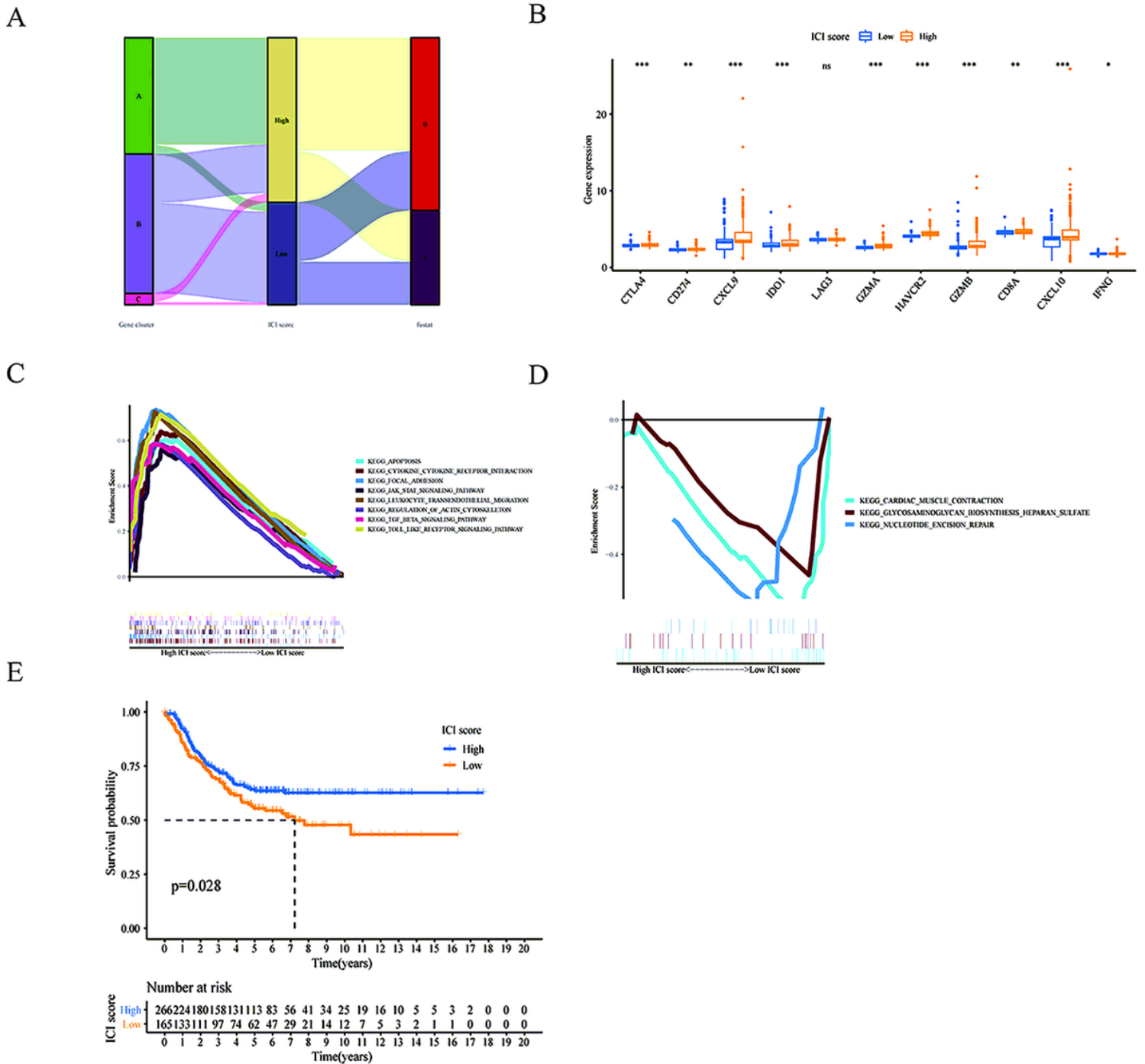


Figure 4

Establishment of ICI score. (A) Distribution of alluvial graph of different ICI clusters, ICI scores and survival status. (B) The expression of immune checkpoint-related targets and immune activation-related targets in different ICI score subgroups. (C) The main enrichment analysis in the low ICI score subgroup was glycosaminoglycan biosynthesis heparan sulfate signaling pathways. (D) The main enrichment analysis in the high ICI score subgroup was apoptosis, cytokine receptor interaction, toll like receptor and leukocyte transendothelial migration signaling pathways. (E) Association between different ICI score groups and overall survival in the TARGET and GSE85047 cohort. Log rank test, $p = 0.028$.